https://doi.org/10.2352/ISSN.2169-4451.2020.36.85

Probabilistic Motion Inference for Fused Filament Fabrication

Francisco Jose Mercado Rivera; Doctoral student; Technologies for Manufacture Research Group (GITEM); Department of Automation and Electronic; College of Engineering; Universidad Autónoma de Occidente; Cali; Valle del Cauca; Colombia.
Alvaro Jose Rojas Arciniegas; Associate professor; Technologies for Manufacture Research Group (GITEM); Department of Automation and Electronic; College of Engineering, Universidad Autónoma de Occidente; Cali; Valle del Cauca; Colombia.
Victor Adolfo Romero Cano; Assistant professor; Remote Command and Distributed Control Systems Research Group (GITCOD); Department of Automation and Electronic; College of Engineering; Universidad Autónoma de Occidente; Cali; Valle del Cauca; Colombia.

Abstract

Additive manufacturing techniques have been the focus of studies and technological advances in recent years, obtaining the capability to fabricate pieces with complex geometries easily, rapid and with high precision, allowing the use of different materials, the appearance of new techniques, and a range of applications beyond prototyping. However, Additive Manufacturing techniques are still affected by some deficiencies and challenges such as the absence of sensing and control during the fabrication process that would result in a more reliable process and printed part. This paper shows the development of an inference process using probabilistic graphical models, in order to track the motion of the extrusion nozzle during the printing process using linear encoders.

Introduction

Additive Manufacturing processes or 3D printing systems consists of generating a three-dimensional object with specific geometry by the successive addition of material in layers [1], [2]. This kind of manufacture requires the computer-aided design to describe the proper geometry of the object. Nowadays, additive manufacturing encompasses different techniques such as [3], [4]: Vat photo polymerization; Material Extrusion; Binder Jetting; Material Jetting; Directed Energy Disposition; Powder Bed Fusion; and Sheet Lamination. Currently, the main differences between these techniques are the raw material used, the states of those materials, and the means to accomplish adhesion between the particles of the material. These techniques provide the versatility to fabricate almost any geometry, reduce costs, and facilitates prototyping which in turns shortens product development time, becoming a particularly attractive alternative for industrial sectors such as aeronautics, automotive, biomedical, education, and health. In general, additive manufacturing processes begin with a computer-aided design (CAD) of the piece or product to make, this design is usually saved as mesh file (.STL) to be processed by a specialized software which is responsible to slice the object transversely in order to reproduce its geometry. The same software generates commands and routines (G-code) for the 3D printer to fabricate the desired object [5]. Figure 1 shows the 3D printing workflow.

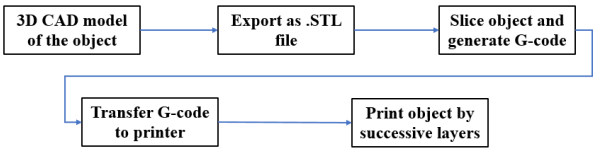

***Figure 1**. 3D printing workflow*

One of the most affordable and popular AM technologies is Fused Filament Fabrication (FFF), which consists in pushing a filament of a thermoplastic material (usually PLA or ABS) through a hot extrusion nozzle onto a printing platform. By generating a relative motion between the nozzle and the printing platform and controlling the push of material, the printer is able to lay down patterns in 2D that forms a layer of the desired object. The printer then adjusts the relative height of the nozzle to the platform and lays down a new layer in the same manner. This process is repeated until the desired tridimensional piece is obtained. It is important to note that before depositing the new layer, the previous layer must already be solidified in order to guarantee a stable surface for the next layer deposition [4], [6]. Figure 2 shows the schematic of the FFF process.

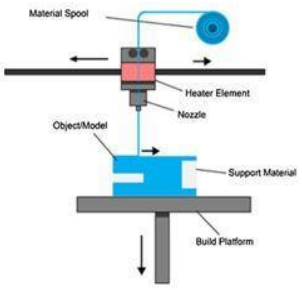

Figure 2. FFF schematic process [7]

However, this technology derived from material extrusion is prone to suffer from several deficiencies and challenges such as the absence of monitoring and control during the fabrication process, materials limitations, uncertainty in the quality of the piece, poor mechanical performance, and several others [8], [9]. These process limitations allow the possibility of errors during the printing process that can be reflected in the objects [10]–[13]. Example of these are layer displacement and incomplete prints (see Figure 3), that go unnoticed during the printing process and result in a defective piece. These failures affect not only the aesthetics and an accurate reproduction of the desired geometry, but also result in poor adhesion between layers, poor mechanical performance, waste of time and material.

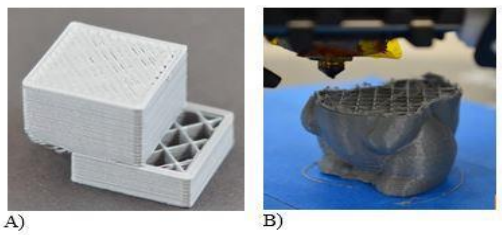

Figure 3. A) Layer displacement error. B) No Material Extrusion error [14].

Most of these printing failures can be attributed to the fact that 3D printers work in open-loop, i.e. 3D printers do not include supervision and control systems for the different variables, and the system cannot detect or correct those deviations from the desired trajectories. Therefore, the development of a closed-loop control system is suggested, in order to track, measure, and control the variables involved in the different additive manufacturing processes and consequently reduce the possibility of failures during the printing process [15]–[20]. The objective of this paper is to develop a supervision system based on Probabilistic Graphical Models in order to observe (and get an accurate information of) the printing process, specifically on how the printer is moving during the printing process, referenced to the G-Code generated through the slicing of the .STL file.

The following section revises relevant related work that set the basis for the work proposed, then a probabilistic graphical model definition is presented, an inference machine is then proposed and some results are presented afterwards. The paper concludes highlighting the potential of this approach to strengthen 3D printing systems by incorporating supervision systems and closing the control loop.

Related Work

There has been increasing research into how to implement numerical models, process monitoring and supervision, and control systems for additive manufacturing. Numerical modeling of the complete process is rare; the work by Xia et.al. in simulations of Fused Filament Fabrication using a front tracking method [21], which uses the finite-volume/front tracking method is an example of these efforts. The experimental validation of a numerical model for the strand shape in material extrusion additive manufacturing [22], investigates the influence of the processing conditions on the cross-section of a printed strand contrasting the results of their numerical model of the process.

The development of sensors for Additive Manufacturing process is also one active research area; Baumann et. al. [23] proposes the concept development of a sensor array for 3D printer, which include sensor for motion/vibration, temperature, orientation and hygrometry. This development is conceived under the premise to be an easily deployable and wireless sensor client-server system.

The implementation of a Closed-Loop Control of a 3D printer Gantry [24] is an example of a research that combines numerical modeling and the implementation of sensors on the printer. This MS thesis developed at Washington University starts by using a low-cost 3D printer in order to explore the advantage of using a closed-loop control in a FFF printer, where magnetic sensors were installed to track the movement in the X, Y, and Z-axis. The information captured by the sensors is processed to control the relative spatial position of nozzle and platform. If an error is detected, based on the G-code for the printing process, the system performs a corrective action.

Similarly, an initial approach to close the control-loop for the positioning of a 3D printer was proposed by Ceron and Rojas [25] in which linear optical encoders were installed along the three axes of a FFF printer. Tests were performed with a basic proportional controller and results confirmed the advantages of closing the control loop for geometry reproduction under various perturbations of the printing process.

3D printing companies have shown interest in creating more robust, closed-loop systems, using different variables (temperature, velocity, flow of material, etc.) to improve the quality of the objects made with their printers. An example is the Polish company ZMorph that manufactures 3D printers with an integrated closed-loop control system [26]. The control system uses angular encoders located at each of the five stepper motors of the printer that provide its angular position. The addition of this closed-loop control system makes it possible to fabricate objects with better surface finishes at high printing speed. However, the use of angular encoders at each motor does leave room for errors since it cannot detect problems with the transmission mechanisms to move nozzle or platform, or even if some of the encoders fail the process would be affected.

Probabilistic Graphical Model Definition

The proposed approach is to track and control the motion of a FFF 3D printer, from a data association generated from an .STL file which describes the geometry of the object to print. The G-code represents the motion to be done by mechanical elements of the printer in order to move the extrusion nozzle and platform along X, Y, and Z axes.

The graphical model is shown in Figure 4, where every X represents a new stage of the nozzle extruder during the printing process, stages which are described by a vector with x, y, z position, and the speed of each axis, and Y_1 correspond to the observation of the stages through sensors. To define the relationship between different stage are proposed a linear motion model and a nonlinear motion model of the dynamic of the printer.

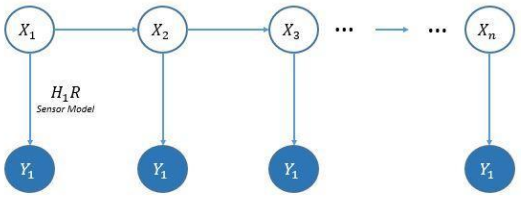

***Figure 4**. Graphical Model.*

Linear Model:

The relationship between different stages are established by Equation (1), where A represents the dynamics between the different stages and P (Equation (2)) is a random variable from a Gaussian distribution which represents an error in the relationship.

$$X_n = AX_{n-1} + P \tag{1}$$

$$P \sim N(\emptyset, V) \tag{2}$$

The projection of the state ahead is described by Equation (1). For this specific application the transition matrix A is defined by a constant velocity transition matrix, assuming that while printing a piece the velocity remains constant throughout the motion expressing a linear dynamic model. This transition matrix A is defined by Equation (3). The error on the transition P can be defined as an identity matrix multiplied by a constant as shown in Equation (4), where L corresponds to the covariance constant.

$$A = \begin{bmatrix} 1 & 0 & 0 & dt & 0 & 0 \\ 0 & 1 & 0 & 0 & dt & 0 \\ 0 & 0 & 1 & 0 & 0 & dt \\ 0 & 0 & 0 & 1 & 0 & 0 \\ 0 & 0 & 0 & 0 & 1 & 0 \\ 0 & 0 & 0 & 0 & 0 & 1 \end{bmatrix} \begin{bmatrix} x \\ y \\ z \\ x' \\ y' \\ z' \end{bmatrix} \tag{3}$$

$$P = L * \begin{bmatrix} 1 & 0 & 0 & 0 & 0 & 0 \\ 0 & 1 & 0 & 0 & 0 & 0 \\ 0 & 0 & 1 & 0 & 0 & 0 \\ 0 & 0 & 0 & 1 & 0 & 0 \\ 0 & 0 & 0 & 0 & 1 & 0 \\ 0 & 0 & 0 & 0 & 0 & 1 \end{bmatrix} \tag{4}$$

These stages are observed by a linear optical encoder (Linear encoder WTB 500 [27]) represented by Y_1 in Equation (5), every position of x, y, and z is sensed by one of these encoders with a resolution of 0.005 mm and the printing speed will be estimated by the variation of these positions. The specifications of these encoders are shown in table 1. The relationship between the stage and the measurements are defined by the Equation (5), where H is a factor that converts the readings of the system into the desired variable and R (Equation (6)) is a random variable from a Gaussian distribution which represent an error in the relationship.

Table 1. Linear encoder WTB 500 specifications

Resolution	0.005 mm
Output Signal	5 V – TTL

Signal Type	Two Quadrature Signal
Velocity	1.2 m/s
Maximal Value Measure	530 mm

$$y_1 = HX_1 + R \tag{5}$$

$$R \sim N(\emptyset, D) \tag{6}$$

In this case, H is defined in Equation (7), representing that the sensors measure the position in the x, y, and z axes as independent variables. Also, the measurements present some error in its values, for that reason the Equation (8) describes a matrix that contains a deviation for each value of a measure, where D corresponds to a constant that depicts this error.

$$H = \begin{bmatrix} 1 & 0 & 0 & 0 & 0 & 0 \\ 0 & 1 & 0 & 0 & 0 & 0 \\ 0 & 0 & 1 & 0 & 0 & 0 \end{bmatrix} \tag{7}$$

$$R = D * \begin{bmatrix} 1 & 0 & 0 \\ 0 & 1 & 0 \\ 0 & 0 & 1 \end{bmatrix} \tag{8}$$

Nonlinear model

The projection of the state ahead is described by Equation (9). In this case the dynamic of the state ahead is represented through a vector function that depends on the last state X_{k-1}, and the control input u. This vector function involves the nonlinearity of the motion dynamic and it is established because of the variations on the position of the extruder and the printing speed during the printing process are nonlinear. For this specific application, only the control input is considered in the vector function and it is described by the G-Code for every movement and speed required during the printing process.

$$X_k = f(x_{k-1}, u_k) = \begin{bmatrix} X_{GCode-k} \\ Y_{GCode-k} \\ Z_{GCode-k} \\ \dot{X}_{GCode-k} \\ \dot{Y}_{GCode-k} \\ \dot{Z}_{GCode-k} \end{bmatrix} \tag{9}$$

These states are observed by the same linear optical encoder presented in the last section, and the relationship between the states and the measurements are defined by the Equation (10) that represents a function of how the sensor observe the stage.

$$y_1 = h(x_k) = \begin{bmatrix} X \\ Y \\ Z \end{bmatrix} \tag{10}$$

Inference Machine

Knowing that the graphical model for tracking the motion of a FFF 3D printer has a tree structure [28] (indicating that in the graphical model there is one and only one path between any pair of nodes, and consequently it has no loops in the structure definition and states [28]) the inference of the states can be obtained by introducing factors in the model structure, Figure 5 shows the new factor graph. This inference can be achieved with the application of a Kalman filter for the linear model, and the application of an extended Kalman filter for the nonlinear model, these are interactive filters composed by two elements: the prediction process and the correction process.

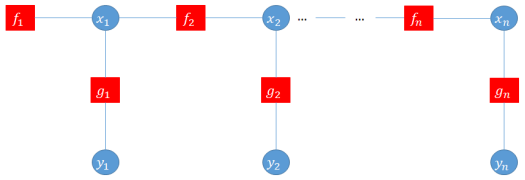

***Figure 5**. Factor graph*

Kalman filter for linear model

The interactive process of the Kalman filter is shown in Figure 6 .

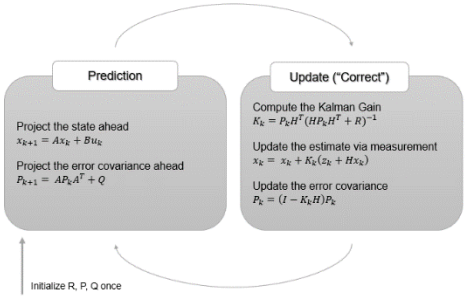

***Figure 6**. Kalman filter process. Adapted from:* [29]

The prediction is the process were the system computes the next state, taking into account the actual state, a transition matrix, and a projection using a covariance error.

Also, the prediction in every interaction computes a new estimation of the covariance matrix, this update is given by the Equation (11) and depends on the transition matrix, the actual estimation of covariance matrix, and matrix denominated Q, which represents a noise in the covariance matrix.

$$P_{n+1} = AP_nA^T + Q \tag{11}$$

The process noise in the covariance Q is determined by Equation (12), were dt is equal to the acceleration of the noise in the process.

$$Q = dt \begin{bmatrix} 1 & 0 & 0 & 0 & 0 & 0 \\ 0 & 1 & 0 & 0 & 0 & 0 \\ 0 & 0 & 1 & 0 & 0 & 0 \\ 0 & 0 & 0 & 1 & 0 & 0 \\ 0 & 0 & 0 & 0 & 1 & 0 \\ 0 & 0 & 0 & 0 & 0 & 1 \end{bmatrix} \tag{12}$$

The correction process of the Kalman filter is given by three elements that are changing with the different interactions. The first element is the computation of the Kalman filter gain; this gain is computed using the observation matrix H, the covariance error matrix of the states P, and the covariance error matrix of the sensor R, as described by Equation (13).

$$K_k = P_kH^T(HP_kH^T + R)^{(-1)} \tag{13}$$

The second element of the correction process is updating the state estimation using the measurement as described by Equation (14), where x_k is the actual state value, K_k is the Kalman gain previously computed, Z_k is the actual measured value and H is the observation matrix.

$$x_k = x_k + K_k(Z_k - Hx_k) \tag{14}$$

The last step of the correction process is the update of the covariance error, this update process is established by Equation (15), and depends on the Kalman gain K, the observation matrix H and the covariance error matrix P.

$$P_k = (I - K_kH)P_k \tag{15}$$

Extended Kalman filter for nonlinear model

The process of the extended Kalman filter is shown in Figure 7.

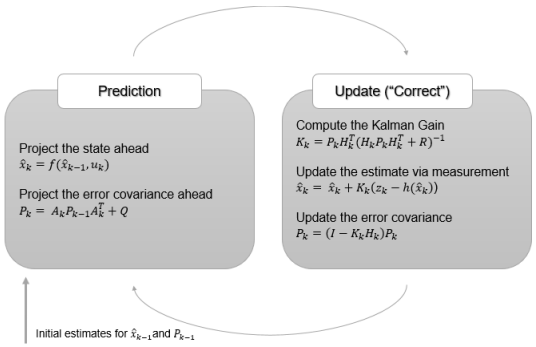

Figure 7. *Extended Kalman filter process. Adapted from:[30]*

The prediction is the process were the system computes the next state, considering that the function depends on the last state and the control input. For this specific case, only the control input is taken into account as the G-Code in every step of the printing process.

The covariance matrix is updated according to Equation (16) where A corresponds to the Jacobian of the states' function as Equation (17) shows, and matrix denominated Q, which represents the process noise in the covariance matrix.

$$P_{n+1} = AP_nA^T + Q \tag{16}$$

$$A = \begin{bmatrix} \frac{\partial f(x_{k-1},u)}{\partial x} & \cdots & \frac{\partial f(x_{k-1},u)}{\partial x} \\ \vdots & \ddots & \vdots \\ \frac{\partial f(x_{k-1},u)}{\partial \dot{z}} & \cdots & \frac{\partial f(x_{k-1},u)}{\partial \dot{z}} \end{bmatrix} \tag{17}$$

However, the Jacobian of the states' function cannot be analytically calculated because, there is not an specific function to describe the dynamic of the states; therefore, this Jacobian matrix is computed in every iteration as the successive differences of the states as shown in Equation (18), allowing to obtain an approximation of the first partial derivatives.

$$A = \begin{bmatrix} \frac{x_k - x_{k-1}}{TimeStep} & \cdots & 0 \\ \vdots & \ddots & \vdots \\ 0 & \cdots & \frac{\dot{z}_k - \dot{z}_{k-1}}{TimeStep} \end{bmatrix} \tag{18}$$

The process noise in the covariance Q is determined by Equation (19), were *dt* is equal to the acceleration of the noise in the process.

$$Q = dt \begin{bmatrix} 1 & 0 & 0 & 0 & 0 & 0 \\ 0 & 1 & 0 & 0 & 0 & 0 \\ 0 & 0 & 1 & 0 & 0 & 0 \\ 0 & 0 & 0 & 1 & 0 & 0 \\ 0 & 0 & 0 & 0 & 1 & 0 \\ 0 & 0 & 0 & 0 & 0 & 1 \end{bmatrix} \tag{19}$$

The correction process of the extended Kalman filter is given by the same three elements. The first element is the computation of the Kalman filter gain, using the covariance error matrix of the states P, the covariance error matrix of the sensor R, and the matrix H as described in Equation (20), but in this case this matrix corresponds to the Jacobian matrix of the observation function as shown in Equation (21).

$$K_k = P_k H^T (HP_k H^T + R)^{(-1)} \tag{20}$$

$$H = \begin{bmatrix} \frac{\partial h(x_k)}{\partial x} & \cdots & \frac{\partial h(x_k)}{\partial x} \\ \vdots & \ddots & \vdots \\ \frac{\partial h(x_k)}{\partial \dot{z}} & \cdots & \frac{\partial h(x_k)}{\partial \dot{z}} \end{bmatrix} \tag{21}$$

Because the observation function is a linear function the result of the Jacobian matrix is equal to the Equation (22)

$$H = \begin{bmatrix} 1 & 0 & 0 & 0 & 0 & 0 \\ 0 & 1 & 0 & 0 & 0 & 0 \\ 0 & 0 & 1 & 0 & 0 & 0 \end{bmatrix} \tag{22}$$

The second element of the correction process is updating the state estimation using the measurement (as described in Equation (23)), where x_k is the actual state value, K_k is the Kalman gain previously computed, Z_k is the actual measured value and $h(x_k)$ is the observation function.

$$x_k = x_k + K_k(Z_k - h(x_k)) \tag{23}$$

The last step of the correction process is the update of the covariance error, this update process is established by Equation (24), and depends on the Kalman gain K, the observation Jacobian matrix H and the covariance error matrix P.

$$P_k = (I - K_k H)P_k \tag{24}$$

Experimental Results

The trajectory established for the experimental process was a square with dimension 50x50x0.6mm and thickness of 0.4mm this represents a printing process with only 3 layers if the layer height is 0.2 mm and a nozzle of 0.4mm is used. Figure 8 shows the shape and the trajectory used for the experimental process. This specific printing process takes 150 s with a set speed of 35 mm/s.

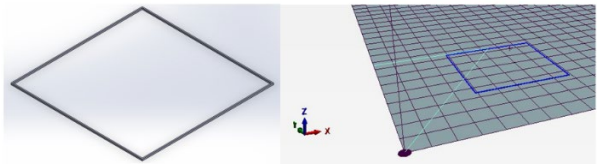

Figure 8*. Shape and printing trajectory*

This trajectory allows to know that there is always movement at least in one axis, furthermore, due to the geometry of the object the motion of an axis (x or y) is null until another trajectory is in process. The z axis only performed the movement when the movement in x and y axis were done. Figure 9 shows the results of the measurements obtained during the printing process.

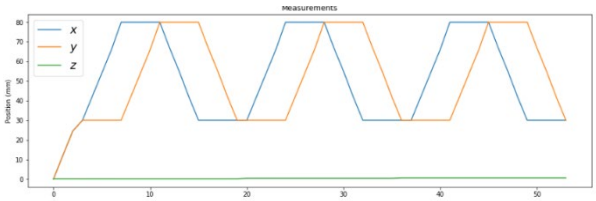

Figure 9. *Measurements obtained by the linear encoders during the printing process.*

Results of the Kalman filter for linear model

First it is necessary to establish some aspects required in the Kalman filter application: a constant velocity of 35 mm/s is defined for the printing process in every axis, in order to use the model of a constant velocity approach.

Another important parameter is the acceleration of process noise required in Equation 10, for this case the acceleration was considered as dt = 0.4 mm/s^2.

Other parameters defined were the constant that affects the covariance transition matrix P, and the covariance observation matrix R; to run these experiments the constant L was defined as

50, and the constant D was defined as 1, this means that the model believes more in the observations than in the transition model.

Once the parameters and the measurements were taken, an algorithm that computed the interactive Kalman filter was used in order to estimate the trajectories. The results are shown in Figure 10, where it can be observed that the estimation of the state does not represent a good estimation of the motion in the printing process.

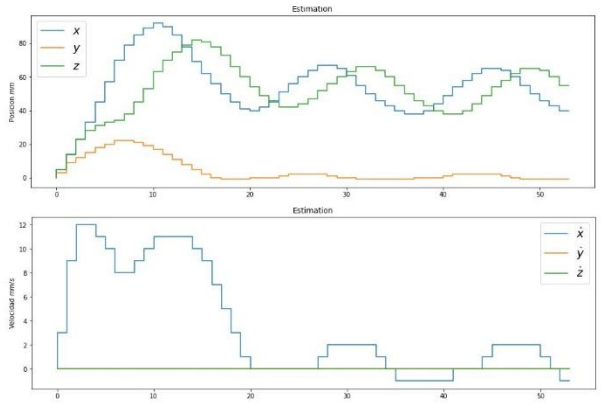

Figure 10. *First estimation results of the Kalman filter.*

Adjustments of the constants L, D, and dt were performed intending to improve the model, setting more weight on the measurements and in this manner the inference process would be more reliable. The new settings were L = 100, D = 1/16, and dt = 1. This process can be done because the system will always have information about the sensor. The results obtained are shown in Figure 11, these results are a better fit to the results and the dynamic of the established trajectory.

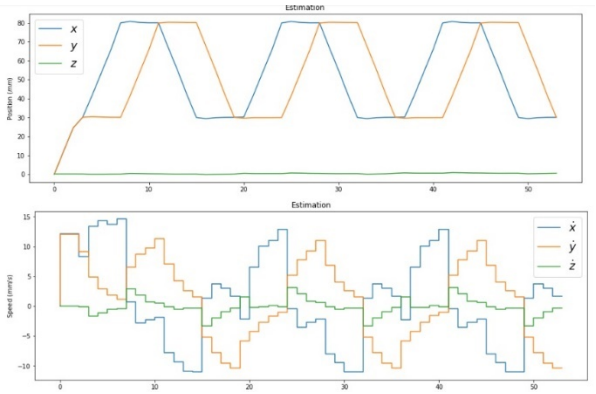

Figure 11. *Second estimation results of the Kalman filter.*

After adjustments of the constants L, D and dt a comparison between the measurements and the states estimation is performed in order to verify the results. Figure 12 shows the measurements of the position obtained in the x axis, and the estimation of the trajectory for x axis, where the estimation mostly fits the trajectory measured by the linear encoders, this means that the inference machine is providing appropriate estimates of the states.

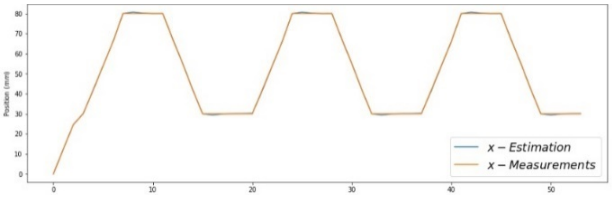

Figure 12*. Comparison between measurements and estimation results in x axis using Kalman filter.*

In order to quantify the error between the trajectory and the estimation through the Kalman filter, the mean square error was calculated for the all 330mm movement done in the x axis, having 5.006 mm as a result, this means that error between the estimation and the trajectory is proximally 1.51%.

Results of the extended Kalman filter for nonlinear model

In order to execute the extended Kalman filter for the nonlinear model is necessary to establish the GCode that's is going to be used as the prediction states function. Figure 13 shows the trajectory established by the GCode during the printing process.

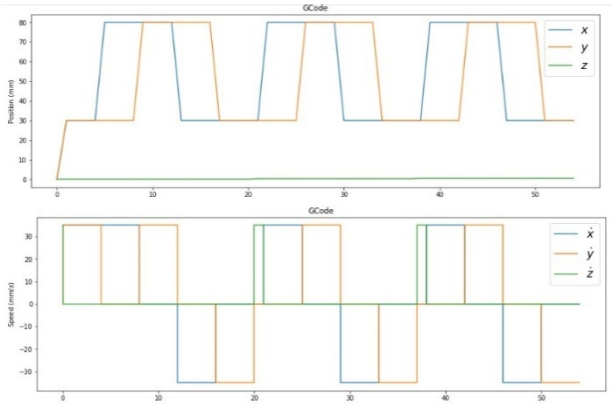

Figure 13. *GCode for the printing process.*

In this case, the parameters where configure different, because now a more realistic model (GCode) can describe the dynamic during the printing process. The new settings were L = 1, D = 1 and dt = 0.0001. This means that we have a good transition model and a good measurement. The results obtained are shown in Figure 14, these results fits to the results and the dynamic of the established GCode trajectory.

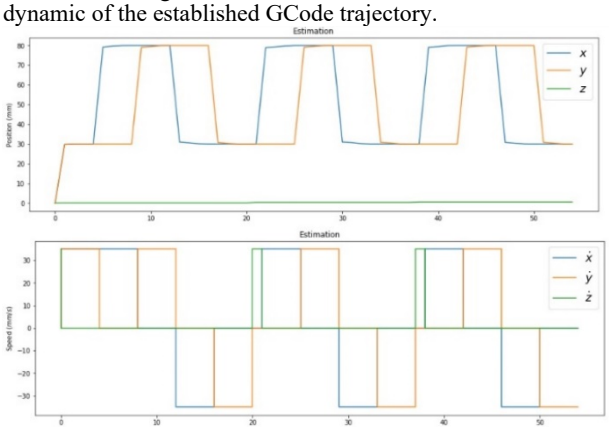

Figure 14*.Estimation results of the extended Kalman filter.*

To quantify the error between the trajectory established by the GCode and the estimation of the extended Kalman filter, the mean square error was calculated for the all 330mm movement done in the x axis, having 5.06 mm as a result, this means that error between the estimation and the trajectory is approximately 1.53%.

Adding noise to the measurements

During the printing process is possible that sensors can be failed or some noise can be introduced to the measurement signal, for that reason to the measurements some gaussian noise where added to simulated an unexpected problem during printing process and see what happens with the estimation with the two different estimation model. The new measurements are shown in Figure 15.

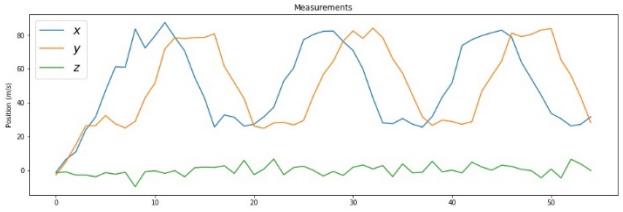

Figure 15. *Noisy measurements.*

The results obtained for the linear model using Kalman filter can be observed in Figure 16, where the estimation of the different states is not a good estimation, this is because the linear model established for this application do not represent a good dynamic for the printing process, and having setup the parameter to believe more in the measurements the Kalman filter does not perform a good estimation process.

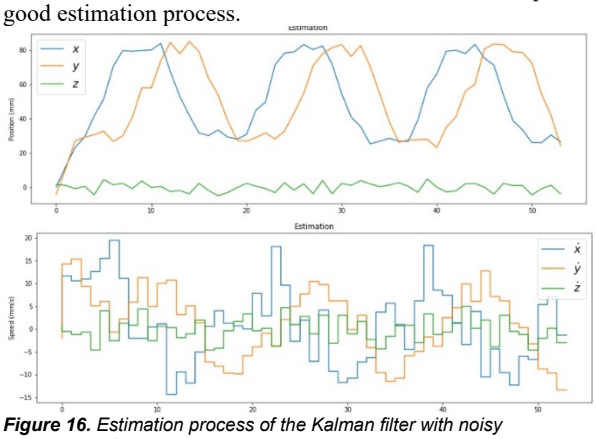

Figure 16. *Estimation process of the Kalman filter with noisy measurements.*

The results for the extended Kalman filter can be observed in Figure 17, where the estimation fits better to the trajectory for the printing process; this happens because this is a more realistic dynamic model using the GCode as the states function. Also, the comparison shows in figure 18 between the noisy measurements for position in x, GCode trajectory for position in x, and the estimation of the x position shows that the extended Kalman filter can produce a good estimation even if something happens with the measurements during the printing process.

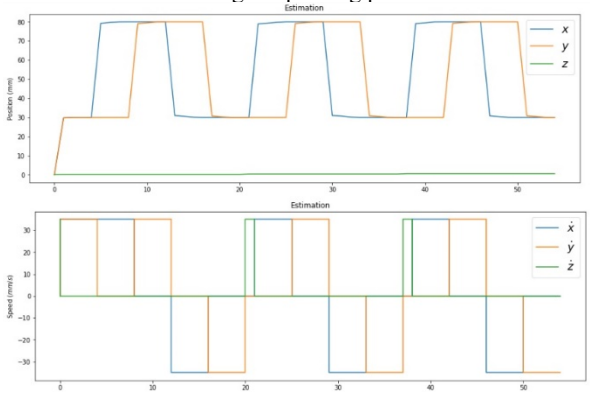

Figure 17*. Estimation process of the extended Kalman filter with noisy measurements.*

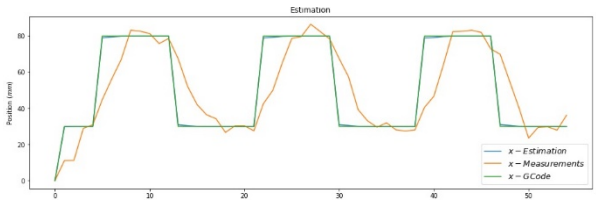

Figure 18*. comparison between noisy measurements, GCode trajectory and estimation for position in* ***x.***

To have another perspective of how the trajectory established by the GCode and the estimation of the states through the extended Kalman filter fits, when some noise is added to the measurements, a plot of the trajectories in the x and y axis was made and can be seen in Figure 19. The difference between the estimation and the GCode is barely noticeable in Figure 19. B.

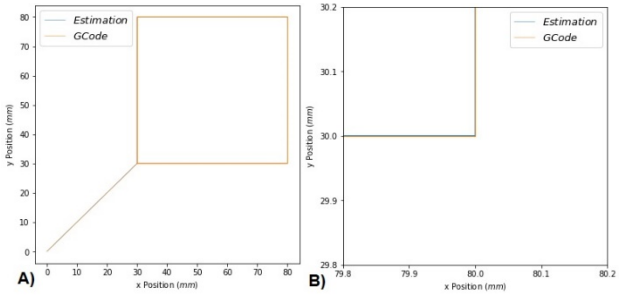

Figure 19. *A) Trajectory in the XY-plane (GCode and Estimation). B) Detail plot of the bottom right corner of the trajectory.*

Discussion

Additive Manufacturing has an interesting potential use in different fields but is still a young manufacturing type which is in constant improvement. One of the challenges it still has is the incorporation of closed-loop control in order to get better performance in the machines and the pieces obtained by these processes, but to achieve this kind of control it is important to develop numerical models, supervision, monitoring, and predictive systems to have information that allows the control system to make accurate decisions during the printing process.

The development of a Probabilistic Graphical Model using as an inference machine a Kalman filter for linear dynamic model, and an extended Kalman filter for nonlinear dynamic model requires the constant iteration between the prediction and the correction stages, in order to guarantee a correct inference value. Also, it is important to know the dynamics of the process to set the parameters for the inference machine.

The Kalman Filter used for the linear dynamic model produced good results with low error for estimating the dynamics of a printing process if the measurement of the states does not present errors. This linear dynamic model does not capture any irregularities in the printing process, thence it was necessary to setup the Kalman filter to follow more the measurements than the dynamic model.

On the other hand, the extended Kalman filter used for the nonlinear model produced good results for estimating the dynamics of a printing process, the GCode was included as a control input for the states function, making the estimation more accurate. Also, this method allows tracking of the system even if the system receive noisy values from the sensors, doing the prediction based in the transition model.

Probabilistic Graphical Models used as an inference method can be a tool for tracking the motion in the 3D printing process, and it can be adjusted to the dynamics of the motion during the process. For future work this inference process can be used as a state observer, allowing to have feedback of the process and to close the control loop over the motion during the printing process. This approach would be an important step to prevent failures and improve the results and piece performance obtained by FFF and could be extended to other additive manufacturing techniques making printers more robust.

The integration between this Probabilistic Graphical Model and an FFF 3D printer is currently being done; this required an improvement in the instrumentation and processor of the 3D printer, in order to obtain the necessary measurements and enough information processing capabilities. This process has extended much longer than anticipated because of the COVID-19 pandemic, the access to the University and the laboratory was restricted for several months and many restrictions are still in place to prevent further spread of the virus.

Reference

[1] I. Gibson, D. Rosen, and B. Stucker, *Additive Manufacturing: Technologies 3D Printing, Rapid Prototyping, and Direct Digital Manufacturing*, Second. New York: Springer.

[2] F. Calignano *et al.*, "Overview on additive manufacturing technologies," *Proc. IEEE*, vol. 105, no. 4, pp. 593–612, 2017.

[3] ISO/ASTM, "ISO/ASTM 52900: Additive manufacturing-General principles-Terminology," 2015.

[4] H. Bikas, P. Stavropoulos, and G. Chryssolouris, "Additive manufacturing methods and modeling approaches: A critical review," *Int. J. Adv. Manuf. Technol.*, vol. 83, no. 1–4, pp. 389–405, 2016.

[5] J. Gardan, "Additive manufacturing technologies: state of the art and trends," *Int. J. Prod. Res.*, vol. 7543, no. August, pp. 1–15, 2015.

[6] R. Jones *et al.*, "Reprap - The replicating rapid prototyper," *Robotica*, vol. 29, no. 1 SPEC. ISSUE, pp. 177–191, 2011.

[7] "FDM setup [243]. | Download Scientific Diagram." [Online]. Available: https://www.researchgate.net/figure/FDM-setup-243_fig5_321702417. [Accessed: 01-Nov-2018].

[8] S. Singh, S. Ramakrishna, and R. Singh, "Material issues in additive manufacturing: A review," *Journal of Manufacturing Processes*, vol. 25. 2017.

[9] D. L. Bourell, M. C. . Leu, and D. W. Rosen, "Identifying the Future of Freeform Processing 2009," *Rapid Prototyp. J.*, p. 92, 2009.

[10] M. Faes *et al.*, "Process Monitoring of Extrusion Based 3D Printing via Laser Scanning," 2016.

[11] P. M. Sammons, M. L. Gegel, D. A. Bristow, and R. G. Landers, "Repetitive Process Control of Additive Manufacturing with Application to Laser Metal Deposition," *IEEE Trans. Control Syst. Technol.*, vol. 27, no. 2, pp. 566–575, 2019.

[12] M. Mani, S. Feng, B. Lane, A. Donmez, S. Moylan, and R. Fesperman, "Measurement science needs for real-time control of additive manufacturing powder-bed fusion processes," *Addit. Manuf. Handb. Prod. Dev. Def. Ind.*, vol. 55, no. 5, pp. 629–676, 2017.

[13] O. Holzmond and X. Li, "In situ real time defect detection of 3D printed parts," *Addit. Manuf.*, vol. 17, pp. 135–142, 2017.

[14] "Print Quality Troubleshootnng Guide." [Online]. Available: https://www.simplify3d.com/support/print-quality-troubleshooting/. [Accessed: 14-Jun-2019].

[15] L. D. Sturm, M. I. Albakri, P. A. Tarazaga, and C. B. Williams, "In situ monitoring of material jetting additive manufacturing process via impedance based measurements," *Addit. Manuf.*, vol. 28, no. February, pp. 456–463, 2019.

[16] N. I. of S. and Technology, "Measurement Science Roadmap for Metal-Based Additive Manufacturing," 2013.

[17] J. S. Batchelder, W. J. Swanson, and K. C. Johnson, "Additive Manufacturing System and Process with Material Flow Feedback Control," 2015.

[18] I. J. S. Batchelder *et al.*, "MODEL GENERATION SYSTEM HAVING CLOSED-LOOP EXTRUSION NOZZLE POSITONING," 1994.

[19] H. LIU, Z. YUAN, and L. Jinfa, "CLOSED-LOOP CONTROL FUSED DEPOSITION MODELING HIGH-SPEED 3D PRINTER AND CLOSED-LOOP CONTROL METHOD," 2016.

[20] R. L. Zinniel and J. S. Batchelder, "Volumetric Feed Control for Flexible Filament," 2000.

[21] H. Xia, J. Lu, and G. Tryggvason, "Simulations of fused filament fabrication using a front tracking method," *Int. J. Heat Mass Transf.*, vol. 138, pp. 1310–1319, 2019.

[22] M. P. Serdeczny, R. Comminal, D. B. Pedersen, and J. Spangenberg, "Experimental validation of a numerical model for the strand shape in material extrusion additive manufacturing," *Addit. Manuf.*, vol. 24, no. September, pp. 145–153, 2018.

[23] F. Baumann, M. Schön, J. Eichhoff, and D. Roller, "Concept Development of a Sensor Array for 3D Printer," *Procedia CIRP*, vol. 51. pp. 24–31, 2016.

[24] B. J. Weiss, "Closed_loop control of a 3D printer Gantry," 2014.

[25] A. J. Rojas Arciniegas and M. Cerón Viveros, "Development of a Closed-Loop Control System for the Movements of the Extruder and Platform of a FDM 3D Printing System," in *NIP & Digital Fabrication Conference, Printing for Fabrication*, 2018, pp. 176–181.

[26] ZMorph, "Closed Loop System in ZMorph 2.0 SX Explained - ZMorph Blog." [Online]. Available: http://blog.zmorph3d.com/closed-loop-system-explained/. [Accessed: 06-Mar-2019].

[27] L. Leader Precision instrument Co., "Linear Encoder for Milling Machine," 2019. [Online]. Available: https://leader-precision.en.made-in-china.com/product/QbXEVLCJHdWG/China-Linear-Encoder-for-Milling-Machine.html.

[28] C. BISHOP, "Pattern Recognition and Machine Learning," *Compstat*. Springer Science+Business Media, LLC, pp. 3–9, 2006.

[29] "Kalman Filter Implementation for Constant Velocity Model (CV) in Python." [Online]. Available: https://github.com/balzer82/Kalman/blob/master/Kalman-Filter-CV.ipynb?create=1. [Accessed: 05-Dec-2019].

[30] "Extended Kalman Filters - MATLAB & Simulink - MathWorks España." [Online]. Available: https://es.mathworks.com/help/fusion/ug/extended-kalman-filters.html. [Accessed: 23-Jun-2020].

Author Biography

Francisco Mercado Rivera received his BS in Mechatronics Engineer from the Universidad Autónoma de Occidente (2017) and nowadays is doing his PhD in the Universidad Autónoma de Occidente. His researches fields are additive manufacturing, product development and control systems.

Alvaro J. Rojas Arciniegas is an associate professor at the department of Automation and Electronics in the College of Engineering of Universidad Autonoma de Occidente in Cali, Colombia. He holds a PhD in Imaging Science from the Chester F. Carlson Center for Imaging Science of Rochester Institute of Technology in Rochester, NY. He holds MS degrees in Industrial Engineering from RIT and in Systems and Entrepreneurial Engineering from University of Illinois at Urbana-Champaign, and a BS in Mechatronic Engineering from UAO. His research interests include Additive Manufacturing, Product and Process Design Methodologies, Control, and Image Processing. He has combined his academic experience with industry work developing projects of technological improvement and innovation.

Victor Romero Cano is an assistant professor and researcher at Universidad Autónoma de Occidente, Colombia. He received his PhD degree from the Australian Centre for Field Robotics at University of Sydney, Australia, in 2015. His research focuses on developing perception systems that are able to describe objects of interest in complex dynamic environments by exploiting the multi-modal nature of sensor data. His research interests include robotic perception, and learning and inference in probabilistic graphical models.